Correlations between Silica Chemistry and Structural Changes in Hydrothermally Treated Hexagonal Silica/Surfactant Composites Examined by in Situ X-ray Diffraction

Adam F. Gross, Van H. Le, Bradley L. Kirsch, Andrew E. Riley, and Sarah H. Tolbert*

Department of Chemistry & Biochemistry, University of California, Los Angeles, Los Angeles, California 90095-1569

Received January 31, 2001. Revised Manuscript Received May 15, 2001

In this paper, the effect of silica chemistry on hydrothermal restructuring of silica/surfactant composites is investigated. The materials were studied using real time X-ray diffraction to follow structural changes in *p*6*mm* hexagonal samples as they were hydrothermally treated in buffers ranging from pH 7 to pH 11. Changes in pore shape, repeat distance, and peak area were found to depend on the treatment conditions. Treatment at pH 11 caused expansion of the lattice, a small amount of pore shape restructuring, and a small increase in diffraction peak area. Treatment in a pH 7 hydrothermal solution, by contrast, resulted in contraction of the lattice, significant pore shape restructuring, and large increases in diffraction peak areas. These changes were correlated with ^{29}Si MAS NMR, which was used to examine changes in framework polymerization, and with liquid ^{1}H NMR, which was used to follow loss of surfactant from the composite. It was found that lattice expansion is facilitated by low framework polymerization and little or no surfactant loss while the opposite conditions were necessary for lattice contraction. The maximum amount of pore restructuring occurred under pH 9 conditions. At this pH, both silica condensation and silica hydrolysis have appreciable rates, suggesting that both processes are necessary for optimum restructuring. Finally, correlations between surfactant loss and changes in overall diffraction intensity indicated that these changes resulted primarily from increased electron density contrast in the material caused by loss of surfactant from the organic domains. The conclusions of this work help explain the molecular basis for the modifications that are commonly observed in X-ray diffraction patterns after hydrothermal treatment of periodic silica/surfactant composites.

Introduction

Hydrothermal restructuring is commonly used to improve the structural characteristics of silica/surfactant composites.[1−6] Understanding the chemistry behind these changes is important to optimize the process and to rationally control the final outcome of the synthesis. Appropriate hydrothermal treatment can result in more ordered and better-condensed materials.[2,3,5] In some materials, a hydrothermal phase transformation also occurs, which may be used to synthesize desired products.[2−4,7−10] Hydrothermal treatment may be performed in both pure water and high-pH synthesis solutions, but different physical changes are reported in the literature depending on whether water or the very basic synthesis solution treatment is used.[2,5,11,12] This observation leads to the obvious conclusion that solution pH must be an important factor in controlling restructuring. This conclusion is supported by the fact that silica chemistry has a strong dependence on pH:[13,14] At neutral pH, silica condensation is fast while the hydrolysis of Si−O−Si bonds is slow. The opposite is true at high pH.

* To whom correspondence should be addressed. E-mail: tolbert@chem.ucla.edu.

(1) Kresge, C. T.; Leonowitz, M. E.; Roth, W. J.; Vartuli, J. C.; Beck, J. S. *Nature* **1992**, *359*, 710. Beck, J. S.; Vartuli, J. C.; Roth, W. J.; Leonowicz, M. E.; Kresge, C. T.; Schmitt, K. T.; Chu, C. T.-W.; Olson, D. H.; Sheppard, E. W.; McCullen, S. B.; Higgins, J. B.; Schlenker, J. L. *J. Am. Chem. Soc.* **1992**, *114*, 10834.

(2) Huo, Q.; Margolese, D. I.; Stucky, G. D. *Chem. Mater.* **1996**, *8*, 1147.

(3) Gross, A. F.; Ruiz, E. J.; Tolbert, S. H. *J. Phys. Chem. B* **2000,** *104*, 5448.

(4) Gallis, K. W.; Landry, C. C. *Chem. Mater.* **1997,** *9*, 2035.

(5) Ryoo, R.; Jun, S. *J. Phys. Chem. B* **1997,** *101*, 317.

(6) Wu, J.; Liu, X.; Tolbert, S. H. *J Phys. Chem. B* **2000,** *104*, 11837.

(7) Chen, X.; Huang, L.; Li, Q. *J. Phys. Chem. B* **1997,** *101,* 8460.

(8) Gross, A. F.; Le, V. H., Kirsch, B. L.; Tolbert, S. H. *Langmuir* **2001**, *17*, 3496.

(9) Kim, M. J.; Ryoo, R. *Chem. Mater.* **1999,** *11*, 487.

(10) Landry, C. C.; Tolbert, S. H.; Gallis, K. W.; Monnier, A.; Stucky, G. D.; Norby, P.; Hanson, J. C. *Chem. Mater.* **2001**, *13*, 1600. Tolbert, S. H.; Landry, C. C.; Stucky, G. D.; Chmelka, B. F.; Norby, P.; Hanson, J. C.; Monnier, A. *Chem. Mater.*, in press.

(11) Kruk, M.; Jaroniec, M.; Sayari, A. *Microporous Mesoporous Mater.* **1999,** *27*, 217.

(12) Kruk, M.; Jaroniec, M.; Sayari, A. *J. Phys. Chem. B* **1999,** *103*, 4590.

(13) Iler, R. K. *The Chemistry of Silica: Solubility, Polymerization, Colloid and Surface Properties, and Biochemistry*; Wiley: New York, 1979.

(14) Brinker, C. J. *Sol-Gel Science: The Physics And Chemistry Of Sol-Gel Processing*; Academic Press: Boston, 1990.

10.1021/cm010100j CCC: $20.00
Published on Web 09/07/2001

An example of practically useful hydrothermal restructuring is the dramatic pore expansion that can occur in some instances. Hexagonal materials heated under hydrothermal conditions in a high-pH solution and at high temperature (150 °C) result in well-ordered large-pore composites.[12,15] This change is apparently caused by chemistry that results in demethylation of the quaternary ammonium surfactant to form a tertiary amine, accompanied by incorporation of a free tetramethylammonium ion into the composite.[12,16,17] The tertiary amine then acts as a swelling agent in the micelles which expands the pores.[18,19] When this same pore enlargement is attempted in water instead of a high-pH solution, only a small increase in pore diameter is observed for moderate heating times.[11] While significant pore expansion does occur in water with very long heating times, the material produced is inhomogeneous. Thus, high pH appears to be necessary to produce the optimum combination of swelling agent and framework flexibility.

It has also been observed that when a variety of hexagonal inorganic/organic composites are hydrothermally heated, the (11)/(20) peak area ratio increases.[2,3,20] The (11)/(20) area ratio also has been observed to increase during the formation of surfactant/inorganic composites.[21−23] Modeling X-ray diffraction patterns from different silica structures leads to the conclusion that this increase in the (11)/(20) ratio is the result of a morphological change in the framework.[20,21,24,25] In one model, the initial, approximately even peak area ratio indicates cylindrical surfactant domains surrounded by a shell of inorganic framework material. These double cylinders are packed on a hexagonal lattice, leaving voids or low-density regions at the intersections of the cylinders. As the material is hydrothermally treated, the voids are filled, and the new composite consists of more hexagonal surfactant domains in a solid inorganic casing.[21,24] Other models similarly postulate a more homogeneous wall density upon hydrothermal treatment, although the details of the condensation that produces this final wall density vary from model to model.[20,25] We will refer to this increase in the (11)/(20) integrated peak area ratio as "annealing" throughout this work. Our previous work, and the work of others, has found that annealing correlates with an increase in the polymerization of the framework.[2,3] Well-annealed, calcined materials are generally quite stable. They can survive treatment in boiling water[5,26] and show both high rigidity and elasticity under extreme isotropic compression.[6]

From the results summarized above, it can be seen that pH, and thus silica chemistry, has a strong effect on structural modification induced by hydrothermal treatment. In this paper, we will systematically investigate these changes by hydrothermally treating silica/surfactant composites using pH-controlled conditions while observing the material with both in situ and ex situ techniques. We note that the material used in the work is a silica/surfactant composite synthesized with a 20-carbon-alkane-tailed trimethylammonium surfactant. Under some pH controlled conditions these materials undergo a hexagonal-to-lamellar phase transition, which we explore in another manuscript.[27] However, the focus of this work will be the structural changes that occur in the hexagonal phase.[2,3] In this paper, the (11)/(20) ratio is tracked to understand the role of pH in annealing. Changes in the (10) peak area and position are followed to determine how pH alters the order and density of the material and to track expansion in the material. Ex situ ^{29}Si MAS NMR is utilized to follow pH-induced changes in polymerization in the composite framework. Finally, ^{1}H NMR, thermogravimetric analysis (TGA), and inductively coupled plasma atomic analysis (ICP) are used to examine any loss of surfactant from the composite and to detect any dissolution of the silica framework. All of these experiments generate a better picture of the relationship between silica chemistry and structural changes that occur in silica/surfactant composites under hydrothermal conditions.

Experimental Section

The synthesis of the silica/surfactant composites used in this work has been described previously.[3] Samples were made with two concentrations of base; low synthesis base concentration (0.150 M) samples are referred to as "more initially interbonded samples", while samples made with higher base concentrations (0.235 M) are referred to as "less initially interbonded samples".[3,28] Control of pH during hydrothermal treatment was achieved using a 0.250 M boric acid/borate buffer. pH 7, 8, 9, 10, and 11 buffers were 0.250 M in H_3BO_3 and 0, 0.042, 0.111, 0.200, and 0.243 M in tetraethylammonium hydroxide, respectively. We note that the pH 7 solution is not a true buffer until some base is released by condensation of the silica framework. In addition, the buffer pH will decrease slightly when heated because of the temperature dependence of the boric acid K_a.[29] Boric acid was chosen because the electron-deficient nature of the borate anion appeared to minimize undesirable chemistry between the anion and the quaternary ammonium surfactant. Less initially interbonded samples treated at a specific pH will be called pH *X* samples (where *X* is the treatment pH), while more initially interbonded samples treated at a specific pH will be called pH *X*c samples (*X* is the pH, and c is for condensed). For example, a pH 9 treated composite made with 0.235 M NaOH will be called a "pH 9" sample, while a pH 9 treated composite made with 0.150 M NaOH will be called a "pH 9c" sample. Both more and less initially interbonded samples were heated at all five pH values.

(15) Sayari, A.; Liu, P.; Kruk, M.; Jaroniec, M. *Chem. Mater.* **1997**, *9*, 2499.
(16) Sayari, A.; Kruk, M.; Jaroniec, M.; Moudrakovski, I. L. *Adv. Mater.* **1998,** *10*, 1376.
(17) Corma, A.; Kan, Q.; Navarro, M. T.; Perez-Pariente, J.; Rey, F. *Chem. Mater.* **1997**, *9*, 2123.
(18) Kruk, M.; Jaroniec, M.; Sayari, A. *Microporous Mesoporous Mater.* **2000,** *35*−*36*, 545.
(19) Sayari, A. *Angew. Chem., Int. Ed.* **2000,** *39*, 2920.
(20) Impéror-Clerc, M.; Davidson, P.; Davidson, A. *J. Am. Chem. Soc.* **2000**, *122*, 11925.
(21) Lindén, M.; Blanchard, J.; Schacht, S.; Schunk, S. A.; Schüth, F. *Chem. Mater.* **1999,** *11*, 3002.
(22) Lindén, M.; Schunk, S. A.; Schüth, F. In *Mesoporous Molecular Sieves 1998*; Bonneviot, L., Béland, F., Danumah, C., Giasson, S., Kaliaguine, S., Eds.; Elsevier: Amsterdam, 1998.
(23) Lindén, M.; Schunk, S. A.; Schüth, F. *Angew. Chem., Int. Ed.* **1998,** *37*, 821.
(24) Schacht, S.; Janicke, M.; Schüth, F. *Microporous Mesoporous Mater.* **1998**, *22*, 485.
(25) Elder, K. J.; Reynolds, P. A.; White, J. W.; Cookson, D. *J. Chem. Soc., Faraday Trans.* **1997**, *93*, 199.
(26) Kim, J. M.; Jun, S.; Ryoo, R. *J. Phys. Chem. B* **1999,** *103*, 6200.
(27) Gross, A. F.; Le, V. H.; Kirsch, B. L.; Tolbert, S. H. *J. Am. Chem. Soc.*, submitted.
(28) Voegtlin, A. C.; Matijasic, A.; Patarin, J.; Sauerland, C.; Grillet, Y.; Huve, L. *Microporous Mater.* **1997,** *10*, 137.
(29) Perrin, D. D. *Dissociation Constants of Inorganic Acids and Bases in Aqueous Solution*; Butterworths: London, 1969.

Structural changes were followed using real time X-ray powder diffraction. Data were collected by heating a slurry of the composite and buffer under a liner temperature ramp. In situ low-angle scattering was collected using 9 keV synchrotron radiation (Stanford Synchroton Radiation Laboratory (SSRL)) and an X-ray CCD camera to time slice the diffraction during heating. The details of the diffraction and heating setup have been presented elsewhere.[3,8,30] Multiple ramp rates were used to examine kinetic effects on annealing. Peaks were fit to Voigt functions to find peak areas and positions.

Composites were characterized by ^{29}Si MAS NMR using a Bruker Avance 300 spectrometer with a standard one-pulse acquisition and a 240 s recycle delay.[3] Samples used for NMR spectroscopy were used as-synthesized or were hydrothermally treated in sealed ampules in a temperature-ramped oil bath.[3] At various temperatures, samples were removed from the bath, rapidly quenched to room temperature, and filtered for NMR analysis as dry powders.

The amount of surfactant expelled from the composite during heating was analyzed using ^{1}H NMR on a Bruker ARX 500 spectrometer with a 4 μs $\pi/6$ pulse and a 300 s recycle delay (due to the presence of micelles in the solution). A solvent suppression routine was used in the pulse program to suppress the water peak. Samples were made by collecting the supernatant from the oil bath heating experiments and mixing these solutions with a standard. For high surfactant concentration samples, deuterated methanol was also added to help break up micelles. The standard was trimethylsilylpropionic acid (2,2,3,3-deuterated) in D_2O. Surfactant concentrations were determined by comparing the triplet from the $-CH_3$ at the end of the surfactant alkane tail ($\sim$0.8 ppm) with the single standard peak ($\sim\angle$0.1 ppm).

ICP analysis for dissolved silica was performed using a Thermo Jarrell Ash Corp. Iris 100. A 1000 ppm Si standard (Aldrich) was used to make calibration standards. TGA experiments utilized a Perkin-Elmer TGA 7 calibrated with alumel, nickel, and perkalloy standards. Samples were heated under nitrogen at a rate of 10 °C/min.

Results and Discussion

Changes in Local Bonding. Composites were heated in buffered hydrothermal solutions to investigate the connection between pH-controlled silica chemistry and nanoscale restructuring of the silica/surfactant composite materials. To do this, we first need to establish the type and extent of local silica chemistry that occurs at each pH. To this end, ^{29}Si MAS NMR spectra were collected on less initially interbonded samples heated under a linear temperature ramp (1.42 °C/min) in an oil bath and then quenched. Figure 1 shows a sample of ^{29}Si NMR spectra obtained on samples heated under different pH conditions to 100 °C. All treated samples were more polymerized than the unheated material, as shown by the Q^4/Q^3 peak area ratio. Q^4 indicates a Si bonded to four other Si atoms through oxygen bridges and represents a fully condensed silica structure. The Q^3 peak indicates three **Si**−O−Si bonds and one terminal **Si**−O^- or **Si**−OH. For these materials, Q^3 Si represents either a defect or part of the very large interfacial area always present in these composites. A sample is the most polymerized when it has the largest Q^4/Q^3 integrated area ratio. Treatment in a pH 11 buffer caused the smallest increase in the Q^4/Q^3 integrated area ratio, while treatment in a pH 7 buffer resulted in the largest increase. There was a monotonically decreasing trend in the Q^4/Q^3 ratio with increasing pH. Numerical values are shown in Figure 2 for the data shown in Figure 1 and for data taken at many other temperatures. At all temperatures, treatment in a pH 7 buffer yielded the most condensed samples while pH 11 treatment yielded the least condensed materials. All samples, however, showed net condensation evidenced by an increasing Q^4/Q^3 ratio with increasing temperature.

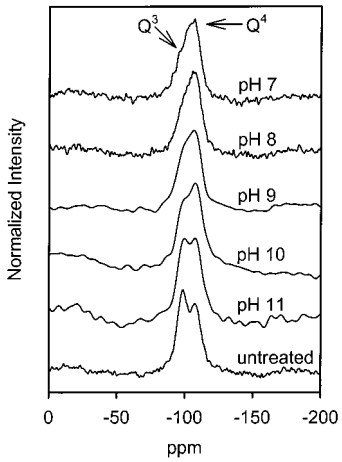

Figure 1. NMR spectra of less initially interbonded samples quenched after heating at different pH values to 100 °C using a ramp rate of 1.42 °C/min. The treatment pH is indicated on the graph. A sample is most polymerized when it has the largest Q^4/Q^3 integrated area ratio. The amount of condensation in the silica framework is observed to follow the trends of silica chemistry. At pH 7, silica shows fast condensation, which results in the most interbonded framework. At pH 11, condensation is slow and little composite polymerization occurs upon hydrothermal treatment.

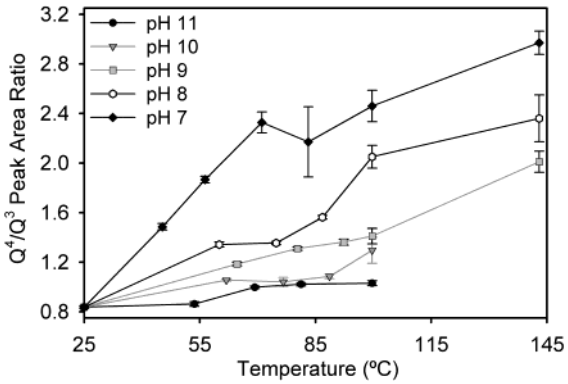

Figure 2. Changes in framework polymerization with temperature for less initially interbonded samples quenched after heating at different pH values using a ramp rate of 1.42 °C/min. The legend shows the treatment pH. Q^4 indicates a Si bonded to four other Si atoms through O bridges, while the Q^3 peak indicates three **Si**−O−Si bonds and one terminal **Si**−O^- or **Si**−OH bond. pH 7 treatment results in the most polymerized framework, while pH 11 treatment results in the least interbonded structure. Intermediate pH values show the expected fan of Q^4/Q^3 ratios.

The results on the composite framework can be compared with what is known about silica chemistry. Silica chemistry changes drastically over the pH range used in this experiment.[13] Condensation is fast at pH 7, but by pH 11, it has slowed drastically. Hydrolysis of Si−O−Si bonds has an opposite trend. At neutral pH, the hydrolysis rate is almost negligible, but at pH 12, silica dissolves rapidly.[13] Overall, the observed trend of monotonically increasing condensation with decreasing pH is consistent with the expected behavior.

(30) Norby, P. *J. Am. Chem. Soc.* **1997**, *101*, 55215. Norby, P.; Hanson, J. C. *Catal. Today* **1998**, 39, 301.

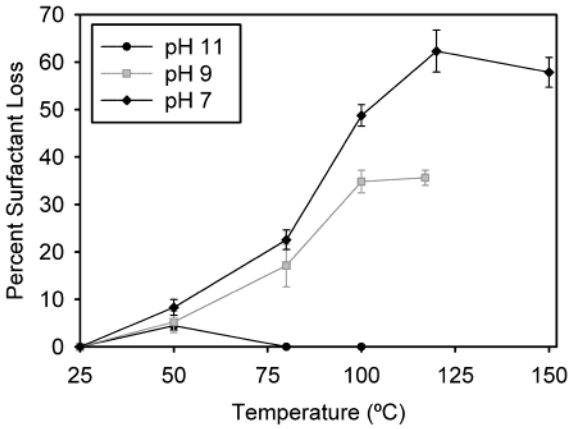

Figure 3. Fraction of surfactant released into solution from less initially interbonded composites as a function of pH and temperature. The legend on the graph indicates treatment pH. Samples were hydrothermally heated at 1.42 °C/min to the desired temperature, quenched, and filtered, and then the supernatant was analyzed for dissolved surfactant using ^{1}H NMR. Data are presented as the percentage of the total composite surfactant found in solution. Silica condensation leads to the largest surfactant loss at pH 7. Less surfactant is lost at pH 9, and the smallest losses result from pH 11 treatment. No surfactant was found above 50 °C for pH 11 treatments, probably due to some surfactant degradation at higher temperatures.

Changes in Composite Composition. Surfactant packing is believed to dominate the observed structures of silica/surfactant composites. Any surfactant that is lost into the hydrothermal solution may thus affect subsequent hydrothermal restructuring. The dramatic increase in silica condensation at low pH shown in Figure 2 provides a route for this loss. When a surface $Si-O^-$ species that is electrostatically bound to a surfactant condenses with another Q^3 species to form two Q^4 species, an OH^- ion can be liberated. If this hydroxide ion diffuses away, the surfactant that was bound to the Q^3 site is also freed and can be expelled into solution. ^{1}H NMR was performed on the supernatant from ex-situ hydrothermal heating experiments (in the oil bath) to measure the amount of surfactant in solution. Figure 3 shows that, for a less initially interbonded sample, pH 7 treatment resulted in the largest amount of expelled surfactant. Treatment at pH 9 resulted in less surfactant lost. Treatment at pH 11 resulted in even less surfactant loss, and at 80 °C and higher, no surfactant was found in solution. The disappearance of surfactant above 50 °C was probably due to Hoffman elimination, which resulted in the demethylation of the quaternary ammonium surfactant to form a tertiary amine and an alkene in strongly basic environments.[12,16,17]

The trend of increasing surfactant loss with decreasing treatment pH was confirmed by TGA experiments on the composites recovered after hydrothermal heating. In these experiments, high-temperature weight loss was used to determine the amount of organic matter remaining in the composite. Samples treated at pH 7, 9, and 11 by ramping the temperature to 80 °C at a rate of 1.42 °C/min showed 16.4 ± 1.5%, 11.1 ± 1.5%, and 0 ± 1.5% surfactant loss by 450 °C, respectively. These numbers are somewhat lower than those obtained from ^{1}H NMR on the solution supernatants probably because rapid ramp rates and an inert gas environment in the TGA prevented complete combustion of the surfactant.

Table 1. Silica Dissolution

pH	supernatant ppm Si	% framework dissolved
7	0 ± 50	0 ± 0.5
9	0 ± 50	0 ± 0.5
11	850 ± 50	4.3 ± 0.5

Table 2. Annealing pH 9 and 11

heating rate (°C/min)	pH 11 maximum (11)/(20) area ratio	pH 9 maximum (11)/(20) area ratio
2.2	1.4	3.0
4.4	1.5	2.9
8.8	1.6	2.8

The results presented in Figures 2 and 3 suggest that condensation-induced surfactant loss may be an important component of hydrothermal restructuring. A question that needs to be answered is whether the surfactant in solution results entirely from condensation-driven surfactant expulsion, or if, instead, some of it results from dissolution of small fractions of the entire composite. To address this question, ICP was also performed on the supernatant from the oil bath based hydrothermal heating experiments to analyze for dissolved silica. Table 1 shows that very little silica was dissolved and released into the hydrothermal solution regardless of treatment pH. In agreement with the basic predictions of silica chemistry, however, high pH did cause the most silica dissolution.

The trends in Table 1 are in agreement with equilibrium silica solubility at high pH.[13] In fact, if composite dissolution at pH 11 is taken into account (Table 1), the average number of Si−O−Si linkages decrease slightly upon hydrothermal treatment (including both Q^3 and Q^4 silica in the framework (Figure 2) and a small amount of presumably Q^0 silica in solution). At pH values other than 11, the ICP data in Table 1 show essentially no silica in solution. Thus, all treatments used allowed the composites to rearrange with only minimal dissolution.

If the solution-phase silica in Table 1 results from complete dissolution of small amounts of composite, some surfactant would be released as well. A comparison of the total amount of dissolved silica (Table 2) and the 50 °C surfactant concentration for pH 11 indicates that these values are, within error, equal to the silica/surfactant ratio of the composite as a whole. Thus, surfactant loss at high pH likely results from complete dissolution of a tiny part of the bulk composite. At lower pH values, however, this surfactant loss cannot be explained by composite dissolution and must result from condensation-driven surfactant expulsion.

As a check on the type of chemistry occurring in solution during hydrothermal heating, the pH of the supernatant from samples hydrothermally treated in an oil bath was also measured for less initially interbonded samples (Figure 4). As discussed earlier, the pH 7 buffer was not a true buffer at the start, but rather a 0.250 M H_3BO_3 solution. During hydrothermal treatment, hydroxide was released due to condensation of the silica framework. This hydroxide reacted with the boric acid to produce a buffer at the very low pH end of the buffer region. As a result of silica condensation, pH 7 buffered solutions show a slow increase in pH. Solutions buffered

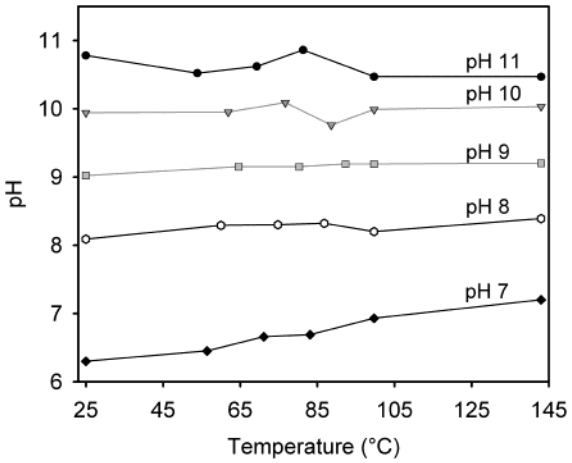

Figure 4. Change in hydrothermal solution pH with temperature for less initially interbonded samples heated at different pH values at 1.42 °C/min and then quenched. The nominal buffer pH is indicated on the graph. All pH values were measured at room temperature after heating to the indicated temperature and then cooling. While pH 8−10 buffers hold their pH well, pH 7 and 11 solutions show some changes. Treatment at pH 7 results in an increase in pH due to silica condensation, while pH 11 treatment results in a small pH drop from consumption of hydroxides during hydrolysis of silica bonds.

between pH 8 and pH 10 hold their pH well, but pH 11 solutions displayed a slight drop in pH with progressive hydrothermal treatment, probably due to consumption of hydroxide from solution during hydrolysis of silica bonds.

Changes in Nanoscale Repeat Distance. The silica chemistry and surfactant loss described above result in a range of changes in structure and diffraction patterns of these composites. The simplest of these changes is an alteration of the periodic repeat distance, which would lead to larger or smaller pores in the calcined silicas derived from these composites. Low-angle X-ray diffraction data were used to observe both expansion and contraction in the materials. Figure 5 shows the lattice constant, *a* (calculated from the diffraction peak positions), as less initially interbonded composites were heated at 4.4 °C/min under different pH conditions. Samples were tracked until they began to undergo a phase transition.

The lattice constant should be affected by silica polymerization, surfactant loss, and surfactant thermal expansion. Silica polymerization leads to a loss of surfactant, which reduces the surfactant volume in the pore. Silica condensation during synthesis of silica/surfactant composites has also been shown to cause reduced lattice spacings, presumably through densification of the silica walls rather than surfactant loss.[31−33] Both mechanisms may be important here. Volume expansion caused by thermal motion of the surfactant alkane tails, by contrast, provides an expansive force in the material. These ideas together explain the changes in lattice parameter presented in Figure 5. Up

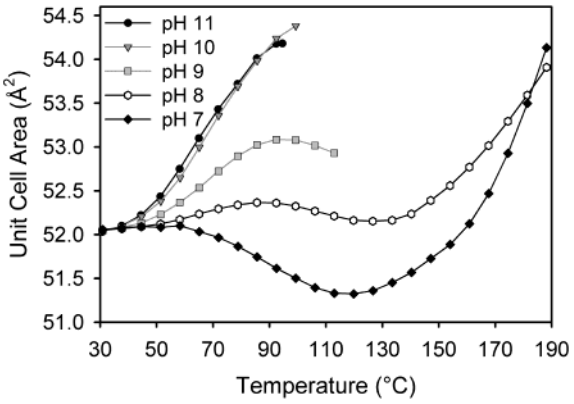

Figure 5. Hexagonal lattice constant versus temperature for less initially interbonded samples heated at 4.40 °C/min in buffered hydrothermal solutions. The legend on the graph shows the buffer pH. High pH samples undergo expansion due to surfactant thermal motion and possibly some decomposition of the surfactant into swelling agents. Composites treated at neutral pH initially contract due to surfactant loss and framework condensation. This is followed by an increase in lattice spacing at higher temperatures caused by surfactant thermal motion and possibly decomposition of the surfactant.

to 120 °C, pH 7 treatment causes a reduced lattice constant. Significant surfactant loss (Figure 3) and silica polymerization (Figure 2) occur up to 120 °C and cause shrinking of the pores. Above 120 °C in a pH 7 buffer, surfactant loss stops (Figure 3), and the lattice constant is observed to increase. Thermal motion of the surfactant tails can apparently dominate structural changes in the composites once surfactant loss has stopped. In addition, some surfactant may decompose into tertiary amines above 150 °C, which are reported to act as swelling agents that further expand the pores.[12,16,17]

By contrast, pH 10 and 11 data show only expansive effects. Little surfactant is lost, and so thermal disordering of the surfactant tails dominates, at even lower temperatures.[8] The low Q^4/Q^3 ratios found in pH 10 and 11 composites may further facilitate this expansion on kinetic grounds. In addition, the high pH may help the small amount of surfactant that is expelled into solution decompose into tertiary amines that could again act as swelling agents.[12,16,17] Finally, it has been suggested that, during high-pH hydrothermal treatments, water enters the palisades region between the surfactant headgroups and swells the organic domains.[34] Thus, a combination of effects probably leads to the pore size expansion seen in Figure 5 for pH 10 and 11 treated samples.

The pH treatments between pH 7 and pH 10 show a mixture of the trends seen in the high- and neutral-pH runs. Treatment at pH 9 shows initial expansion followed by a contraction at 100 °C. Less surfactant is lost at pH 9 compared to pH 7, allowing thermal disorder to create a greater expansive force. The small contraction above 100 °C may be understood in terms of silica polymerization; there is a large jump in the Q^4/Q^3 ratio from 100 to 143 °C (Figure 2) which could shrink the lattice slightly. Changes in the lattice constant of composites heated in a pH 8 solution can be explained in a similar manner. Treatment at pH 8 causes much

(31) Lindén, M.; Ågren, P.; Karlsson, S.; Bussian, P.; Amenitsch, H. *Langmuir* **2000,** *16*, 5831.
(32) Ågren, P.; Lindén, M.; Rosenholm, J. B.; Blanchard, J.; Schüth, F.; Amenitsch, H. *Langmuir* **2000**, *16*, 8809.
(33) Ågren, P.; Lindén, M.; Rosenholm, J. B.; Schwarzenbacher, R.; Kriechbaum,; Amenitsch, H.; Laggner, P.; Blanchard, J.; Schüth, F *J. Phys. Chem. B* **1999**, *103*, 5943.
(34) Khushalani, D.; Kuperman, A.; Ozin, G. A.; Tanaka, K.; Garces, J.; Olken, M. M.; Coombs, N. *Adv. Mater.* **1995,** *7*, 842.

less polymerization and presumably less surfactant loss than pH 7 treatment (Figure 2). As it turns out, for this sample, surfactant thermal disordering and surfactant losses almost cancel out, creating a nearly invariant lattice constant with increasing temperature. At higher temperatures, thermal motion of the surfactant and/or surfactant degradation again dominates, producing a very large lattice expansion like that seen in pH 7 samples at high temperatures.

We note that the same general results are seen regardless of the heating ramp rate. For example, the same spread in lattice constants below 130 °C is seen when a less initially interbonded sample is heated at 2.2 °C/min, compared to the 4.4 °C/min data show in Figure 5. With the slower ramp, however, more time exists for surfactant to decompose at pH 7 and 8, and so a slightly larger high-temperature lattice constant is observed. For example, a pH 7 sample heated at 4.4 °C/min has a lattice constant of 54.1 Å at 188 °C, while a pH 7 composite heated at 2.2 °C/min has a lattice constant of 54.9 Å at that same temperature.

Changes in Pore Geometry. While changes in peak position (and thus periodic repeat distance) are the easiest to quantify, other changes in nanoscale structure also occur under hydrothermal conditions. Examples of structural changes that affect the composite diffraction pattern are shown in Figure 6 (top). The diffraction patterns shown were taken on a less initially interbonded sample heated in a pH 9 buffer. The relative intensity of the (11) and (20) diffraction peaks changes, the overall peak areas increase, and, as discussed above, the peak positions shift. Our goal is now to understand these other structural changes.

The increase in the (11)/(20) peak area ratio can be understood in terms of a transformation from inhomogeneous silica walls with voids or low-density regions to a hexagonal network with a higher, homogeneous wall density.[20,21,24,25] Figure 6 (bottom) shows the change in peak area ratio with temperature for less initially interbonded composites heated at 4.40 °C/min. All of the ratios are fairly constant and close to 1 at low temperatures, but then veer linearly upward around 70 °C. The main difference between the various pH values in Figure 6 (bottom) is that composites heated under high-pH conditions stop annealing at a relatively low temperature and thus show less total change compared to those heated at more moderate pH values. The (11)/(20) area ratio of pH 11 composites levels off first (∼90 °C) at a value of ∼1.5. Composites heated at pH 10 level off at ∼95 °C with a higher (11)/(20) ratio of about 2, while pH 7−9 materials anneal even more. The greatest extent of annealing, with a (11)/(20) ratio equal to 2.9, is found under pH 9 conditions at ∼120 °C. The maximum (11)/(20) values for pH 7 and 8 materials are lower than those for pH 9, but higher than those for pH 10. We note that while the exact (11)/(20) ratio is slightly affected by the ramp rate, the trends discussed above are general and are observed at all thermal ramp rates (see Table 2). As a result, it appears reasonable to make comparisons between the slower heating oil bath heating experiments, which give information about changes in atomic scale bonding, and the slightly faster ramp XRD experiments, which tell us about the nanoscale periodicity in these materials.

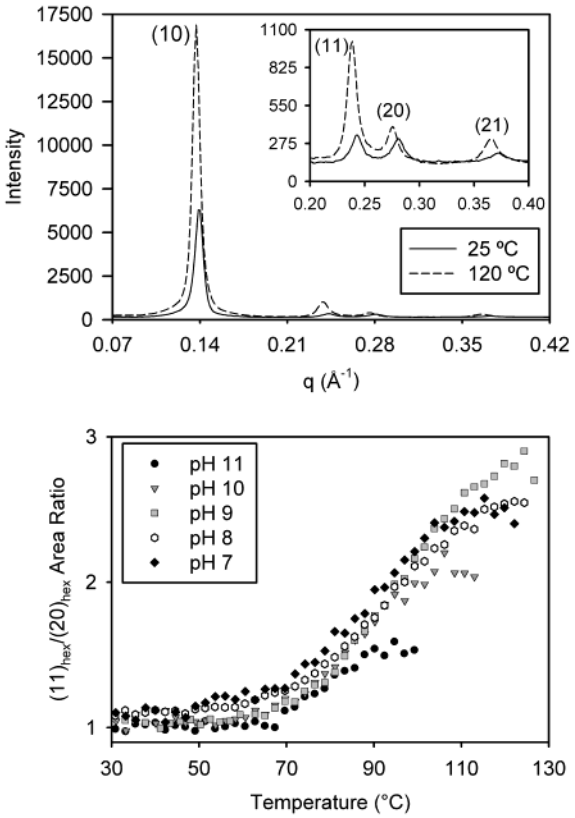

Figure 6. (Top) XRD patterns of a less initially interbonded composite at room temperature and after heating to 120 °C at 4.40 °C/min in a pH 9 buffer. The legend is on the graph, and peak indexing is indicated. (Bottom) The effect of pH on the (11)/(20) peak area ratio for less initially interbonded composites illustrates the dependence of annealing on silica chemistry. The legend is on the graph, and all samples were heated at 4.40 °C/min. At pH 11, conditions where silica condensation is not favored, the material anneals the least. Condensation is more favorable at pH 10, and more annealing is observed. Treatment at pH 7−9, conditions that strongly favor silica polymerization, results in the most change. The most annealed material, however, results when both condensation and some hydrolysis can occur at pH 9.

Since annealing, as we have defined it, is a transformation from silica walls with some low-density regions to more homogeneous, dense walls, silica condensation must be coupled to annealing. A detailed understanding of the relationship between these structural changes and silica condensation may be obtained by comparing the data in Figures 2 and 6 (bottom). pH dependent trends in condensation shown in Figure 2 are related to, but not identical to, trends in annealing shown in Figure 6 (bottom). The most striking difference is that condensation begins immediately upon heating while there is a temperature range where no annealing occurs. The most straightforward correlation is that, under conditions where little condensation occurs, less annealing also occurs (pH 10 and 11) and, under conditions where significant condensation occurs (pH 7−9), the most annealing is also observed. A monotonic trend of increasing extent of annealing with lower pH is not, however, observed; pH 9 treated samples anneal more than pH 7 or 8 treated samples. This can be explained by postulating that the morphological change that we describe as annealing requires some hydrolysis to occur optimally. If only condensation occurs, strain will build into the framework and eventually further distortion

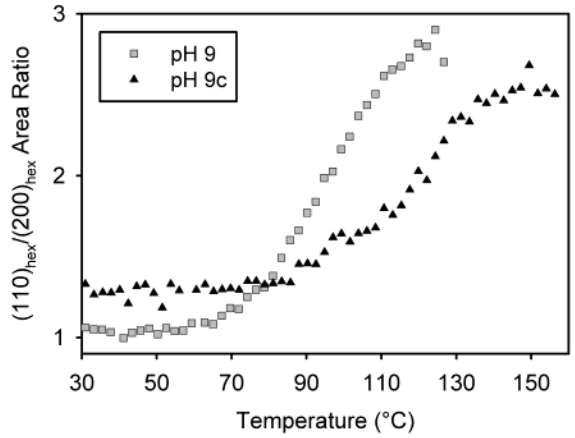

Figure 7. The (11)/(20) peak area ratio versus temperature is shown for composites that are initially more (pH 9c) and less (pH 9) interbonded. Both samples were heated at 4.40 °C/min and treated in a pH 9 buffer. The more initially interbonded sample, pH 9c, starts more annealed, but shows less change and requires higher temperatures to reach the maximum extent of annealing. The more flexible framework in the pH 9 sample allows for greater rearrangement.

of the lattice will become impossible. With some hydrolysis possible, however, high-energy strained bonds can be broken, and the more flexible lattice will be able to maximally reorganize.

Small changes in annealing caused by room-temperature chemistry can also be seen in Figure 6 (bottom) at 30 °C. All of the experimental runs were performed on the same original sample. However, it can be seen that, as a result of exposure to the hydrothermal liquid, the pH 11 treated sample starts out the least annealed ((11)/(20) = 1.01 ± 0.02) while the pH 7 ((11)/(20) = 1.10 ± 0.04) and pH 8 ((11)/(20) = 1.11 ± 0.02) treated samples start slightly more annealed. All errors are 95% confidence intervals. Compared to shifts in (11)/(20) peak area ratios observed at higher temperature, these changes are minor; however, they are statistically significant and reinforce the idea that both silica condensation and small structural changes occur even at low temperature.

In addition to comparing the effect of treatment pH, we can investigate the effect of initial polymerization on the restructuring of the framework. Figure 7 shows the results of heating more and less initially interbonded samples at pH 9. The pH 9c sample starts out more annealed (with a higher (11)/(20) peak area ratio), but does not show as much change as the pH 9 sample. In the end, the pH 9c sample ends up slightly less annealed than the pH 9 sample. Higher temperatures, however, are required to reach the maximum extent of annealing in the pH 9c sample. Even at these higher temperatures (where hydrolysis is faster[13]), there appears to be insufficient hydrolysis to optimally restructure the framework, emphasizing the importance of hydrolysis in annealing. The same trend is found at all pH values with higher temperatures required to reach maximum annealing in more initially interbonded samples. For example, in a pH 7 buffer where almost no hydrolysis occurs, the less initially interbonded pH 7 composite anneals ~20 °C lower than the pH 7c material. There is also a greater difference in the extent of annealing (pH 7 maximum 2.5, pH 7c maximum 1.9), reinforcing the importance of some hydrolysis in annealing.

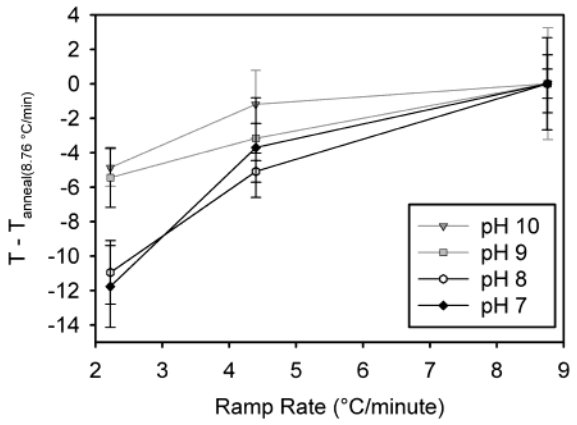

Figure 8. Annealing onset point versus heating ramp rate for less initially interbonded samples treated at different pH values. The legend on the graph shows the treatment pH. All data are shown as the temperature difference between the annealing onset temperature at the fastest ramp rate and the annealing onset temperature at slower ramp rates. pH 7 and 8 treatments show the largest change in annealing onset temperature with heating rate, indicating lower activation barriers to annealing under low-pH conditions where silica condensation is favored.

Beyond examining the extent of annealing, we can also chart the temperature where the (11)/(20) peak area ratios start to rise. The temperature at which annealing begins is found by fitting a line to the minimally sloped data before the ratio increases and another line to the increasing data after the (11)/(20) peak area ratio begins to rise. We define the intersection of these two lines as the onset temperature. Figure 8 shows the effect of the heating rate on the annealing onset for less initially interbonded composites. To make the data easier to follow, all data are charted as the change in onset temperatures relative to the temperature determined for the fastest ramp rate. We have shown in earlier work that when composites are heated in water, the annealing onset temperature will drop with slowing ramp rate, indicating a kinetically limited process.[3] As a result, by examining the annealing onset temperatures at different ramp rates, we can explore the kinetics of the annealing process.

In Figure 8, we observe that the annealing onset always occurs at a lower temperature when the ramp rate is decreased and that data collected at pH 7 and 8 show the largest change in annealing onset with ramp rate. The variation in annealing onset point with ramp rate is a measure of the reaction rate and is related to the activation energy for the process.[3,35] Large changes in annealing onset with ramp rate indicate a low-barrier process, while small changes in annealing onset with ramp rate result from a large activation barrier. These data indicate that annealing under pH 7 or 8 conditions is a rapid, lower activation barrier process while the activation barrier associated with annealing at pH 9 or 10 is higher.[35] However, we believe numerical activation energies calculated from these data are not meaningful because the annealing onset temperatures are determined by the pH-dependent silica condensation rates, but are monitored by observing changes in nanometer scale order. Such a complex kinetic scheme is not well

(35) Ozawa, T. *Bull. Chem. Soc. Jpn.* **1965,** *38*, 1881.

described by the simple equations used for nonisothermal kinetics. Treatment at pH 7 does cause the largest shift in annealing onset point with ramp rate, a fact that reinforces the idea that the kinetics of annealing is facilitated by silica condensation.

Overall, the data presented here indicate that silica condensation and structural change both occur over a wide range of temperatures. Some condensation and minor structural changes can occur near room temperature, while other condensation does not occur until higher temperatures. Annealing occurs predominantly at higher temperature. To unite these observations, we postulate that the majority of polymerization at lower temperatures occurs along the silica/surfactant interface rather than within the silica walls. This is reasonable since there is a high hydroxyl density along the silica/surfactant interface and thus there should be a fairly low activation barrier to this type of condensation. This idea is in agreement with the observed data because condensation along the walls should not significantly change the higher order peak area ratio, but should allow surfactant to be expelled from the composite. Supporting this idea, Figure 3 shows that surfactant is expelled into solution at a fairly constant rate below 100 °C in both pH 7 and 9 treated samples. At higher temperatures, surfactant loss in both the pH 7 and 9 treated samples eventually stops. Since condensation is still occurring at these higher temperatures (Figure 2), we postulate that most of this condensation occurs within the silica walls. Therefore, a general trend exists where condensation occurs mainly along the pore walls at lower temperatures followed by condensation occurring within the silica walls as the material is able to overcome the activation barriers for restructuring at higher temperatures.

These different silica reactivity regions are especially clearly separated at pH 11. Figure 2 shows small but measurable increases in silica condensation as composites are heated at pH 11. Figure 3 indicates that surfactant is released into solution at 50 °C, but that no more surfactant is detected above this temperature. As discussed previously, the disappearance of surfactant above 50 °C is most likely due to base-catalyzed degradation of the surfactant. If, however, surfactant were continually released at higher temperatures, enough should remain to be detected by ^{1}H NMR. That suggests that any condensation at the silica/surfactant interface at pH 11 occurs only at low temperature. At higher temperatures a small amount of annealing is observed starting at ~70 °C (Figure 6), but at this temperature, no free surfactant is found in solution (Figure 3). Thus, all higher temperature condensation probably occurs within the silica walls.

Changes in X-ray Contrast. While relative peak intensity changes provide information about the local geometry around each lattice site, overall changes in peak area contain information about the long-range regularity of the pores and about the X-ray contrast in the material. Significant increases in diffraction peak intensity following hydrothermal treatment have been reported in the literature with little explanation.[5,15,36] Figure 9 tracks these changes with temperature (2.2 °C/min heating rate) using the (10) peak areas for less initially interbonded composites. Treatment at pH 7 causes the (10) peak area to increase dramatically; less change is observed with increasing pH. This same trend is observed regardless of the ramp rate. Similarly, Figure 10 compares changes in (10) area for more and less initially interbonded composites heated at the same pH (pH 9). A much larger increase is observed for less initially interbonded composites than for more initially interbonded materials, a trend that is observed regardless of treatment pH. In all cases, materials that undergo significant condensation show the largest increases in diffraction peak area.

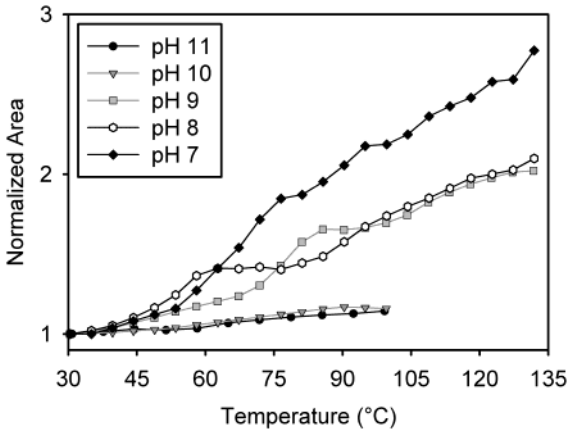

Figure 9. Hexagonal (10) peak areas versus temperature for less initially interbonded samples heated at 2.22 °C/min at different hydrothermal pH values. The legend is on the graph, and all peak areas were normalized to 1.0 at the beginning of the run. pH 7 shows the largest increase in (10) peak area, while comparatively little change is observed at pH 10 or 11. Increased peak area indicates a greater electron density contrast in the material and/or a more regular framework.

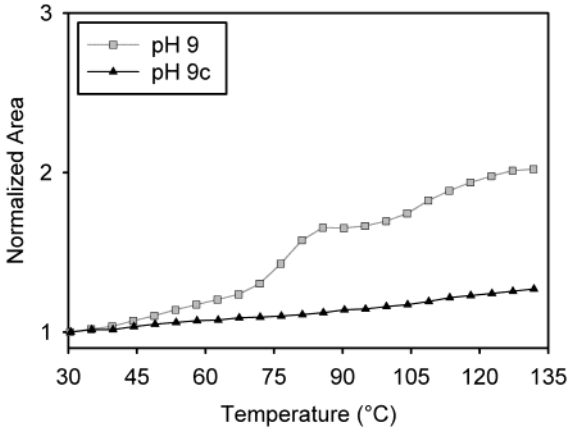

Figure 10. Hexagonal (10) peak areas versus temperature for more (pH 9c) and less (pH 9) initially interbonded samples heated at 2.22 °C/min in a pH 9 buffer. The legend is shown on the graph, and both peak areas were normalized to 1.0 at the beginning of each run. The gain in the (10) peak area for the less initially interbonded sample (pH 9) is accompanied by significant surfactant loss, while the more initially interbonded sample loses almost no surfactant and has a much smaller increase in peak area.

Changes in diffraction peak intensity (Figures 9 and 10) are caused by changes in electron density contrast and variations in long-range regularity of the material. Larger periodic differences in electron density result in more intense scattering peaks.[37] In our silica/surfactant materials, the increased contrast can result from a loss

(36) Elder, K. J.; White, J. W. *Chem. Mater.* **1997**, *9*, 1226.

Table 3. Silica Condensation and Surfactant Loss at pH 9

synthesis [OH^-] (M)	Q^4/Q^3 (25 °C)	Q^4/Q^3 (100 °C)	surfactant loss (%)
0.235	0.84 ± 0.01	1.41 ± 0.06	34.8 ± 2.3
0.150	1.01 ± 0.02	1.34 ± 0.04	1.5 ± 1.5

of surfactant or from an increase in silica wall density. Indeed, a dramatic increase in peak intensity is seen when composites are calcined (where the surfactant is removed and the silica wall density increases).[3] The other morphological change that can alter X-ray peak intensities is a change in the regularity of the periodic lattice.[37] Small variations in the periodic repeat distance will decrease the diffraction peak intensity. Theoretically, the peak area will not change; intensity will simply be shifted to broad, low wings of the peak.[37] In practice, however, broad wings disappear into the baseline, and the peak area does appear smaller for more disordered materials. Examining changes in (10) peak area (Figures 9 and 10) along with silica condensation (Figure 2) and surfactant loss (Figure 3) can help determine the cause of peak area changes in these composite materials.

More initially interbonded samples treated at pH 9 show a very small change in (10) peak area with temperature, while less initially interbonded samples show a 100% increase in (10) peak area. We will first look at factors that cause differences in electron density and then examine changes in regularity. As shown in Table 3, low and high synthesis pH composites start out with different Q^4/Q^3 ratios, but when treated in a pH 9 buffer to 100 °C, they end up with nearly the same degree of silica condensation. Less initially condensed samples, therefore, show a slightly greater change in silica wall density.

A much more dramatic difference, however, is the amount of surfactant lost from the internal organic domains. Almost no surfactant is lost from the material synthesized at low pH, while approximately one-third of the organic phase is removed from the material synthesized at higher pH. We thus postulate that surfactant loss is the dominant factor contributing to the dramatic increase in (10) peak area for the less initially interbonded sample shown in Figure 10. We note that, even though a negligible amount of surfactant is lost in pH 9c treated samples and very little framework condensation occurs, a small increase in (10) peak area is still observed. Since improved X-ray contrast cannot simply explain this rise, this rise in pH 9c composites may be the real result of reduced lattice variation. Figures 3 and 9 help confirm this idea. Treatment of less initially interbonded samples at pH 7 produces the greatest increase in (10) peak area (Figure 9) and also causes the most surfactant loss (Figure 3). Treatment of less initially interbonded samples at pH 9 results in less surfactant loss than that at pH 7 and also a lower increase in (10) peak area. Hydrothermal treatment at pH 11 causes very little surfactant loss and almost no change in (10) peak area. In fact, the change in (10) area at pH 11 is almost identical to that observed for the pH 9c sample (Figure 10) and may also be caused by reduced lattice variation. From the data presented in Figure 9, however, it can be seen that surfactant loss has a much greater effect on diffraction peak areas than reduced lattice variation, and thus it should not be assumed that hydrothermal treatment that results in dramatically increased diffraction intensity has also created more ordered materials.

(37) Kittel, C. *Introduction to Solid State Physics*; Wiley: New York, 1996; pp 34, 48, and 631−633.

Conclusions

We have shown that pH-driven silica chemistry can be used to control structural changes in silica/surfactant composites heated under hydrothermal conditions. The degree of silica polymerization, which controls surfactant loss and framework flexibility, determines whether a material expands or contracts. Surfactant loss near neutral pH results in net contraction. When condensation-driven surfactant loss is prohibited at high pH, thermal disorder of the surfactant tails can swell the pores. Middle-pH conditions (pH 9) create materials with the most homogeneous walls. Neutral-pH conditions, however, lead to the most polymerized materials.

To optimally reorganize the structure of a material, it is best to start with a less polymerized framework. The extent of heating may also be used to control reshaping of the framework. When a material is heated, condensation occurs first at the silica/surfactant interface and then in the interstitial voids. Thus, low-temperature hydrothermal treatment may be used to eliminate surfactant from the pores without altering the framework, while hydrothermal treatment at temperatures greater than ∼70 °C is necessary to restructure the silica matrix. Finally, dramatic changes in peak intensity can be observed which do not correlate with actual structural rearrangements, but rather with surfactant loss. Changes in silica condensation or in relative diffraction peak intensities are better measures of real atomic- and nanometer-scale structural rearrangements.

We note that the trends observed in this work should apply not only to hexagonal silica/surfactant composites synthesized here, but more generally, to a wide range of self-organized silica-based materials synthesized under alkaline conditions. It may also be possible to extend these ideas to non-silica-based composites by drawing parallels between their framework chemistry and the silica chemistry presented here. Using these ideas about the microscopic effects of various treatment conditions, we hope that the tuning of synthetic and postsynthetic parameters for optimal hydrothermal restructuring may become easier. In addition, this work provides insight into interpreting X-ray diffraction patterns from hydrothermally treated composites in terms of fundamental chemical processes.

Acknowledgment. We thank M. J. Strouse for help with NMR spectroscopy. R. L. Garrell and K. Sheran are gratefully acknowledged for help with ICP and TGA, respectively. This paper includes data collected at the Stanford Synchrotron Radiation Laboratory, which is operated by the Department of Energy, Office of Basic Energy Sciences. This work made use of equipment supported by the National Science Foundation under Grant DMR-9975975. This work was supported by the National Science Foundation under Grant DMR-9807190. S.H.T. is an Alfred P. Sloan Foundation Research Fellow.

CM010100J